Huang, Bingkun; Yang, Shimi; Hu, Enyi; Li, Xiuxiu; Wang, Jun; Lund, Peter

Theoretical study on melting of phase change material by natural convection

Published in:
Case Studies in Thermal Engineering

DOI:
10.1016/j.csite.2021.101620

Published: 01/12/2021

Document Version
Publisher's PDF, also known as Version of record

Please cite the original version:
Huang, B., Yang, S., Hu, E., Li, X., Wang, J., & Lund, P. (2021). Theoretical study on melting of phase change material by natural convection. *Case Studies in Thermal Engineering*, *28*, Article 101620.
https://doi.org/10.1016/j.csite.2021.101620

Case Studies in Thermal Engineering 28 (2021) 101620

Contents lists available at ScienceDirect

Case Studies in Thermal Engineering

journal homepage: www.elsevier.com/locate/csite

Theoretical study on melting of phase change material by natural convection

Bingkun Huang [a], Shimi Yang [a], Enyi Hu [a], Xiuxiu Li [a], Jun Wang [a,*], Peter Lund [a,b,**]

[a] Jiangsu Provincial Key Laboratory of Solar Energy Science and Technology, Southeast University School of Energy and Environment, No. 2 Si Pai Lou, Nanjing, 210096, PR China
[b] School of Science, Aalto University, P.O. Box 15100, FI-00076, Aalto (Espoo), Finland

ARTICLE INFO

Keywords:
Latent heat storage
Melting mathematical model
Natural convection
PCM
Coordination factor

ABSTRACT

Natural convection plays a crucial role in latent heat storage system. Determining how natural convection affects the melting of phase change material (PCM) will provide a better understanding of the melting process and give helpful advice on strengthening techniques. The research content of this paper is a mathematical model is established to explain the melting process of PCM affected by natural convection. The mathematical model of phase change melting process is given by introducing the natural convection and the temperature gradient. A coordination factor (Co) based on the mathematical model, which is an instantaneous quantity and proportional to the heat exchange rate and the intensity of natural convection, is introduced to explain the melting process. A square-shaped and shell-tube (concentric, eccentric) PCM heat storage unit were numerically analyzed in more detail. It is found that the Co factor is closely related to the melting rate. It will not promote the melting rate when Co less than 0 while it will promote the melting rate when Co higher than 0, and the higher the Co value, the faster the melting rate. This model gives a clear and quantitative explanation for the problem of melting interface movement affected by natural convection, as well as that increasing the heating temperature and changing only the shape of the heat storage unit can greatly enhance the heat storage rate in this study. The model also provides theoretical guidance for the study of the phase change heat storage enhancement.

1. Introduction

Thermal energy storage utilizing phase change materials (PCMs) have potentially high energy storage density, show efficient performance in almost constant temperature, and are easily available over a broad range of melting temperatures [1–8]. Thermal energy is stored in a material as latent heat upon melting, whereas the stored energy is utilized later when needed by freezing the material [9]. PCMs are already used in several applications such as ventilation [10], refrigeration [11], buildings [12], hot water tanks [13], etc. The main drawback with most solid-liquid PCMs is their inherently low thermal conductivity, which varies between 0.1 and 0.2 W/m K for organic PCMs, and 0.4 and 0.6 W/m K for other PCMs [14]. A low thermal conductivity adversely affects the performance, e.g. increases the recovery times and decreases the storage response time to properly meet the application requirements

---

* Corresponding author.
** Corresponding author. Jiangsu Provincial Key Laboratory of Solar Energy Science and Technology, Southeast University School of Energy and Environment, No. 2 Si Pai Lou, Nanjing, 210096, PR China.
E-mail addresses: 101010980@seu.edu.cn (J. Wang), peter.lund@aalto.fi (P. Lund).

https://doi.org/10.1016/j.csite.2021.101620
Received 24 September 2021; Received in revised form 21 October 2021; Accepted 31 October 2021

Nomenclature

T	Temperature (K)
T_s	Temperature of solid zone of PCM (K)
T_l	Temperature of liquid zone of PCM (K)
T_∞	Heating temperature (K)
T_{solid}	Solid temperature(K)
T_{liquid}	Liquid temperature(K)
Q	Heat absorbed from liquid zone at the wall (J)
c_p	Specific heat capacity at constant pressure (J/kg·K)
$\overrightarrow{\overline{\nabla T_l}}$	Dimensionless temperature gradient
U_∞	Maximum velocity(m/s)
$\overrightarrow{U}$	Velocity (m/s)
$\overrightarrow{\nabla T_l}$	Temperature gradient (K/m)
$\overrightarrow{\overline{U}}$	Dimensionless velocity
Re_x	Reynolds number
Pr	Prandtl number
Nu_x	Nusselt number
P	Static pressure (Pa)
$\overrightarrow{g}$	Gravitational acceleration (m/s^2)
$\overrightarrow{F}$	External body forces
S	Volumetric heat source term
h	Sensible enthalpy (J/kg)
ρ	Density (kg/m^3)
∇	Hamiltonian operator
τ	Stress tensor
δ_t	Thickness of temperature boundary layer (m)
u	Velocity in X-direction (m/s)
v	Velocity in Y-direction (m/s)
E	Energy (J)
t	Time (s)
ΔH	Latent heat (J/kg)
L	Latent heat (J/kg)
Greek letters	
Φ	Heat introduced/leading-out by heat conduction (J)
λ	Thermal conductivity (W/m·K)
μ	Dynamic viscosity (Ns/m^2)
β	Liquid fraction
Subscripts	
s	Solid phase of PCM
l	Liquid phase of PCM

[15].

To improve the performance of PCM thermal storage systems [16], several measures have been recommended [17–20]: increasing the heat transfer surface [17], improving the uniformity of heat transfer process [18], and improving the thermal conductivity of PCM [19]. However, these measures often increase the complexity of the storage system and could have other adverse effects on the thermal performance [21], which usually sacrifices the heat storage capacity or makes it more difficult for industrial processing, or increases the cost of heat storage. For example, nano-additives such as Al_2O_3, Cu and Fe_2O_3 are widely used for the sake of improving the thermal conductivity of PCM, besides, fin shape and arrangement become more and more complex [17,22,23].

Another important research point is about natural convection, which also exists in latent heat storage system enhanced by nano-additives or fins. The effect of natural convection in the melting process of PCM has been previously investigated [24,25], indicating that it could have an important role in the phase melting process, whereas pure conduction leads to poor performance [26,27]. Natural convection at the melting layer has been shown to enhance heat transfer from heat transfer fluid to PCM [24]. Simulations with a cylindrical annulus with PCM found that enhancements of the Rayleigh number increased the heat transfer rate [25], whereas melting in the bottom section was ineffective because most of the heat was transferred to the upper section. Joybari et al. [28] is assumed that natural convection contributes only to the upper half of the storage unit until its liquid fraction value reaches unity. Many researchers focus on the influence of natural convection during melting process. Eccentric tubes were widely studied and they concluded that with increasing the eccentric distance, the area dominated by natural convection dominated increases [29] and the melting rate increases sharply and reduces the melting time [30,31]. Natural convection melting in a square cavity was investigated in literature [32,33] and concluded that variation in boundary conditions had appreciable impact on the natural convection process and melting behavior. The effect of natural convection in microencapsulated PCM slurry [34] system and PCM-metal foam [35] system were also studied, microencapsulated PCM slurry give the best thermal control due to the thermal enhancement of natural convection [34] and the time required for complete melting was significantly reduces because of natural convection [35].

Although these results clearly indicated the different influence of natural convection on the melting process of PCMs in different system, but their conclusions are limited to their results explanations because they did not point out why the enhancement of natural convection can enhance the heat transfer, and did not point out which locations in the latent heat storage system were enhanced by natural convection, for example, natural convection influences melting by flow velocity, where the higher the flow velocity the better the strengthening effect. Therefore, this content aim to find the commonness of the melting process of natural convection in different models, study which parameters in natural convection play an important role in the melting process of phase change materials, and extract the key parameters in the melting process of phase change materials affected by natural convection.

In order to solve the problems of complicated heat transfer enhancement, lack of theoretical guidance of natural convection, lot of literature are read to investigate the problem. Our approach employs two theoretical frames: the theory of the temperature boundary layer and the field synergy principle [36], because author have found that there is a great similarity between the PCM melting scene and the heat transfer of a flat plate outside the fluid. The former theory is related to the temperature difference between the flowing liquid and the solid phase surface, which also produces a thin layer with a sharp temperature change which can be regarded as a temperature boundary layer. The reason why this concept is introduced is that the distant heat flux has no direct heating effect on the melting of PCM, the heat source of the solid phase PCM should be the adjacent liquid phase fluid. The latter theory is linked to reducing the intersection angle between the velocity and temperature gradient, which can effectively enhance convective heat transfer in single-phase heat transfer. It has been widely verified and applied for single-phase heat transfer [37,38], but is rarely used for PCM melting processes. The theory is introduced because the similarity between the PCM melting and the heat transfer of a flat plate outside the fluid.

In this paper, a mathematical model of the PCM melting process is presented to a give the basic method enhancing the heat transfer in latent heat storage. In order to verify the model, the ANSYS FLUENT [39] and TECPLOT tools are employed to explain the detail.

2. Mathematical models

In the next, the mathematical model of energy for the interface between liquid zone and solid zone are described. The following assumptions commonly used in the literature [40,41] are made:

- Flow of liquid PCM corresponds to incompressible Newtonian fluid flow;
- Viscous dissipation is neglected as no large velocity gradients are present;
- Phase-wide constant thermophysical properties are used at different temperatures;
- The first layer of solid microelement at the interface is at melting temperature
- Heat conduction in x-direction is neglected.

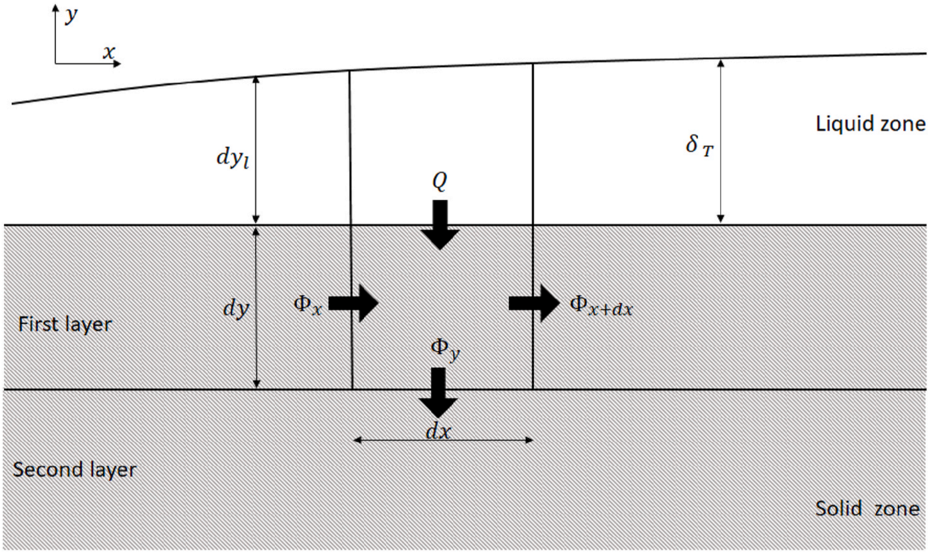

Fig. 1. Temperature and heat flow in boundary layer.

The energy balance of a solid microelement (dz = 1) shown in Fig. 1 can be written as

$$\Phi_x = \Phi_{x+dx} = 0 \tag{1}$$

$$\Phi_y = \lambda_s \left(\frac{\partial T_s}{\partial y} \right) dx \tag{2}$$

where Φ_x stands for by heat conduction in first layer, λ_s is the thermal conductivity of solid PCM, T_s is temperature in the solid zone.

The heat absorbed by the solid-phase microelement from the liquid boundary layer is Q, which is obtained from the heat conduction through the boundary layer:

$$Q = \lambda_l \left(\frac{\partial T_l}{\partial y} \right) |_{y=w} dx \tag{3}$$

where Q is heat absorbed from the liquid zone at the wall, λ_l is thermal conductivity of liquid PCM, T_l is temperature of the liquid zone, subscript “y = w” represents the surface of a solid.

Eq. (3) can be re-written using the field synergy principle [36] as follows:

$$\lambda_l \left(\frac{\partial T_l}{\partial y_l} \right) |_{y=w} = \int_0^{\delta_t} \rho_l c_{p,l} \left(u \frac{\partial T_l}{\partial x} + v \frac{\partial T_l}{\partial y} \right) dy_l \tag{4}$$

where δ_t is the thickness of temperature boundary layer, ρ_l is the density of liquid PCM, $c_{p,l}$ is the specific heat of liquid PCM, u is the velocity in x-direction in liquid zone, v is the velocity in y-direction in liquid zone, dy_l is the length of liquid microelements in y-direction.

The heat absorbed by the solid-phase microelements from the liquid boundary layer can further be expressed as:

$$Q = \left(\int_0^{\delta_t} \rho_l c_{p,l} \left(u \frac{\partial T_l}{\partial x} + v \frac{\partial T_l}{\partial y} \right) dy_l \right) dx \tag{5}$$

The energy balance of microelements could be expressed as:

$$\frac{\partial E}{\partial t} = \left(\int_0^{\delta_t} \rho_l c_{p,l} \left(u \frac{\partial T_l}{\partial x} + v \frac{\partial T_l}{\partial y} \right) dy_l \right) dx - \lambda_s \left(\frac{\partial T_s}{\partial y} \right) dx \tag{6}$$

where E is the energy of a solid microelement including sensible heat and latent heat, t is the time.

The energy E of the solid microelement is associated to two aspects: Physical properties, conditions of velocity and temperature gradient in the temperature boundary layer, and thermal conductivity and temperature gradient in the solid zone.

Therefore, Eq. (6) gives the energy equation of solid-liquid interface and its influencing factors, from Eq. (6), improving the thermal conductivity of the solid material only (under the condition that the external boundary layer condition is unchanged), does not necessarily accelerate the melting process of the solid phase, because the increase of the thermal conductivity of the solid phase and the temperature gradient inside the solid phase also changes. This might be one reason why nano-additives do not always accelerate melting except for the change of viscosity of materials caused by nano-additives, but increase the energy storage capacity. Arasu et al. [41] concluded that in case of 5% nano-additives and a 71% liquid fraction more heat is stored compared to a case with 0% nano-additives and 74% at t = 3000s, which indicates that more sensible heat is stored with 5% of nano-additives.

In vector form, the energy equation on the side of the liquid boundary layer is the following:

$$Q = \int_0^{\delta_t} \rho_l c_{p,l} \left(u \frac{\partial T_l}{\partial x} + v \frac{\partial T_l}{\partial y} \right) dy_l = \int_0^{\delta_t} \rho_l c_{p,l} \left(\overrightarrow{U \cdot \nabla T_l} \right) dy_l \tag{7}$$

where ∇ is Hamiltonian operator, $\overrightarrow{U}$ is the velocity, $\overrightarrow{\nabla T_l}$ is the temperature gradient.

Introducing dimensionless parameters in Eqs. 8–10 below, Eq. (7) can be written in dimensionless form in Eq. (11):

$$\overrightarrow{\overline{U}} = \frac{\overrightarrow{U}}{U_\infty} \tag{8}$$

$$\overrightarrow{\overline{\nabla T_l}} = \frac{\overrightarrow{\nabla T_l}}{\frac{T_\infty - T_l}{\delta_t}} \tag{9}$$

$$\overline{y} = \frac{y_l}{\delta_t} \tag{10}$$

$$\int_0^1 \left(\overrightarrow{\overline{U}} \cdot \overrightarrow{\overline{\nabla T_l}} \right) d\overline{y} \cdot \mathrm{Re}_x \cdot \mathrm{Pr} = Nu_x \tag{11}$$

$$\mathrm{Re} = \frac{\rho u D}{\mu}$$

$$\mathrm{Pr} = \frac{\mu c_p}{\lambda}$$

where $\overrightarrow{U}$、 $\overrightarrow{\nabla T_l}$、 $\overline{y}$ is the dimensionless velocity, temperature gradient and temperature boundary layer positions, respectively, U_∞ is the maximum velocity, T_∞ is the heating temperature, Re_x, Pr and Nu_x are the local Reynolds, Prandtl number and Nusselt number, respectively. It is worth noting that the Re_x is a value just reflecting the flow state of the local position, and is not independent of the Reynolds number in forced convection.

The magnitude of the local Nusselt number reflects the melting rate at current position. Nu_x can be increased by increasing the local Reynolds number, Prandtl number, and the value of the integral in Eq. (11). Without an energy source which can change the Reynolds number, such as a mixing device, Re_x can be regarded as a fixed value. Pr is generally constant in the case of a phase change material. Therefore, we obtain the factors affect the Nu_x, increasing the integral value would be an effective way to improve Nu_x. According to Eq. (11), the vector product of velocity and temperature gradient is proportional to the *Nu* number. Therefore, we define a coordination factor Co representing the state of heating or cooling of a site:

$$Co = \overrightarrow{U} \cdot \overrightarrow{\nabla T} \tag{12}$$

When $Co > 0$ means that hot fluid flows into the unit volume along the temperature gradient or cold fluid flows out along the

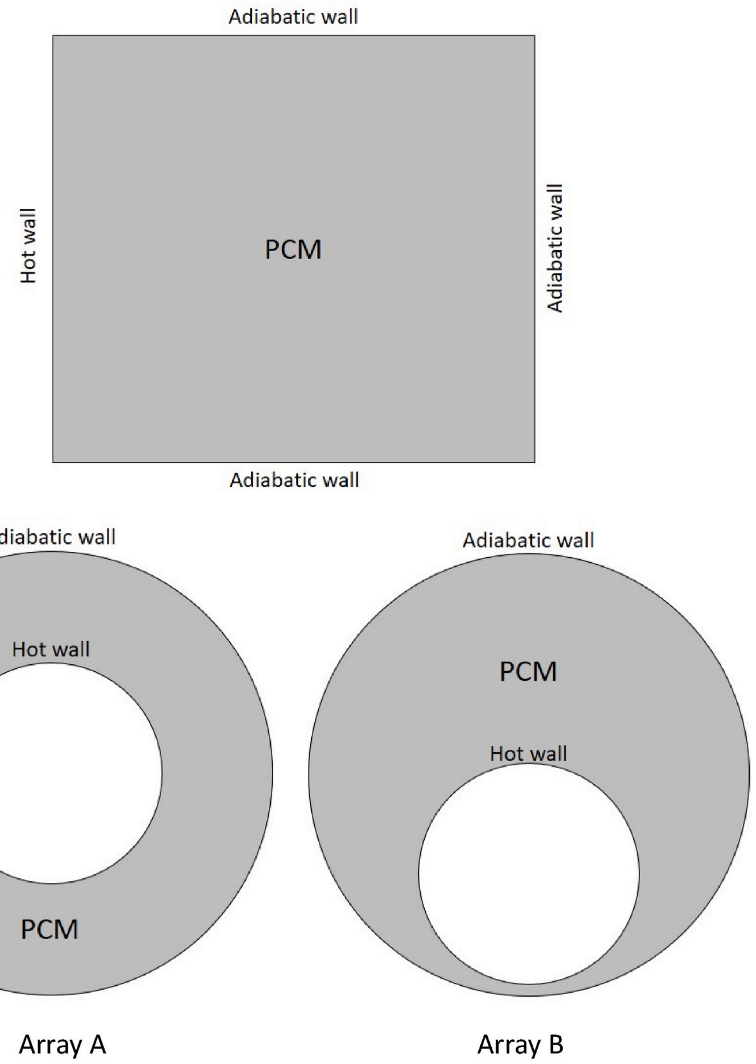

Fig. 2. (a). Square-shape enclosure. (b). Shell-tube unit.

temperature gradient, that is, the unit volume is heated; if $Co \leq 0$ means that hot fluid flows out of the unit volume along the temperature gradient or cold fluid flows into the unit volume along the temperature gradient, that is, the unit volume is cooled.

Although the definition of Co factor comes from the temperature boundary layer, there are also flow mixing of hot and cold fluids in the liquid zone. Therefore, the Co factor is also valid in the liquid zone besides the temperature boundary layer. In the liquid zone, the magnitude of Co indicates the intensity of heating or cooling, that is, the heat transfer strength; while the range of Co indicates the intensity of mixing of hot and cold fluids, that is, the intensity of natural convection.

3. Numerical simulation model

To verify the mathematical model described in Section 2, a numerical study was conducted using the commercial software ANSYS FLUENT 16.0 [42].

3.1. Physical model

Square enclosure and shell-tube are two common classical models, and they have been widely study in literature [29–32,41]. Hence, this two different geometries are used for verification showing in Fig. 2(a) and (b). Fig. 2(a) is a square enclosure of size 40 mm × 40 mm. Fig. 2(b) is a shell-tube unit with an inner diameter of 30 mm and outer diameter 60 mm, respectively. The cylinders are concentric in array A; and the center-to-center distance is 14 mm in array B. Paraffin is selected as the PCM in the square enclosure while N-eicosane is selected as the PCM in the shell- tube unit (their thermophysical properties are origin from Refs. [30,43] respectively, and shown in Table 1). Paraffin [43] and N-eicosane [30] are selected as PCM and they have the same square and shell-tube heat storage units in their corresponding references (see Fig. 3) (see Table 2).

3.2. Governing equations

In the numerical study, the flow is considered unsteady, laminar, incompressible, and two-dimensional. The viscous dissipation term is considered negligible. The viscous incompressible flow and the temperature distribution are solved using the Navier–Stokes and thermal energy equations, respectively. Consequently, the continuity, momentum, and thermal energy equations can be expressed as follows [41]:

Continuity:

$$\frac{\partial \rho}{\partial t} + \nabla\left(\rho \overrightarrow{U}\right) = 0 \tag{13}$$

Momentum:

$$\frac{\partial}{\partial t}\left(\rho \overrightarrow{U}\right) + \nabla \cdot \left(\rho \overrightarrow{U}\overrightarrow{U}\right) = -\nabla P + \rho \overrightarrow{g} + \nabla \cdot \tau + \overrightarrow{F} \tag{14}$$

where P is the static pressure, τ is the stress tensor, and $\rho \overrightarrow{g}$ and $\overrightarrow{F}$ are the gravitational body force and external body forces, respectively.

Thermal energy:

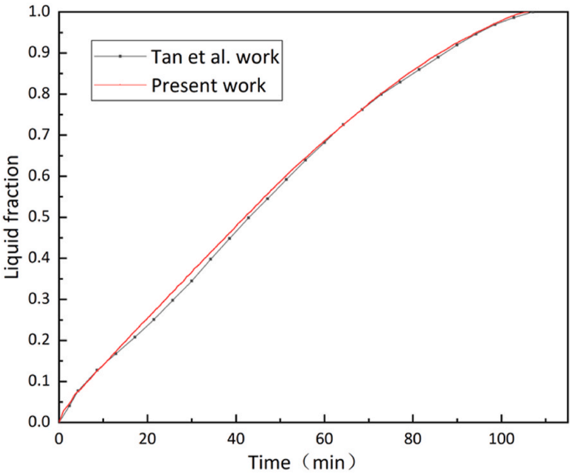

Fig. 3. Comparison of liquid fraction versus time between present study and Tan et al. [45].

Table 1
Properties of paraffin [43] and N-eicosane [30] PCM.

Property	Paraffin	N-eicosane
Density (kg/m^3)	900	770
Specific heat (J/kgK)	2950	2460
Thermal conductivity (W/mK)	0.2699	0.1505
Viscosity (Ns/m^2)	0.03	3.85×10^{-3}
Thermal expansion coefficient (1/K)	0.0005	0.0009
Latent heat (J/kg)	205600	247600
Solid temperature(K)	329	308
Liquid temperature(K)	333	310

Table 2
Initial temperature and boundary conditions for different models.

Model	Initial temperature	Boundary conditions
Square-shaped enclosure	310 K	353 K, 373 K
Shell-tube	298 K	338 K

$$\frac{\partial(\rho H)}{\partial t} + \nabla \cdot \left(\rho \vec{U} H\right) = \nabla \cdot (\lambda \nabla T) + S \tag{15}$$

where H is the enthalpy of the PCM, T is the temperature, ρ is the density of the PCM, λ is the thermal conductivity of the PCM, $\vec{U}$ is the velocity and S is the volumetric heat source term, which is equal to zero here. The total enthalpy H of the PCM is computed as the sum of the sensible enthalpy h and the latent heat ΔH. The latent heat ΔH is

$$\Delta H = \beta L \tag{16}$$

where L is the latent heat, β is the liquid fraction and is defined as

$$\beta = 0 \ if \ T < T_{solid}$$

$$\beta = 1 \ if \ T > T_{liquid}$$

$$\beta = \frac{T - T_{solid}}{T_{liquid} - T_{solid}} \ if \ T_{solid} < T < T_{liquid} \tag{17}$$

For the initial conditions and boundary conditions, the following values are used:

- In the square-shaped enclosure and shell-tube, the temperature of the PCMs are 310 K and 298 K in the beginning, respectively.
- In the square-shaped enclosure, the heating temperature is constant 353 K and 373 K. In the shell-tube, the heating temperature of the inner tube is maintained at 338 K.

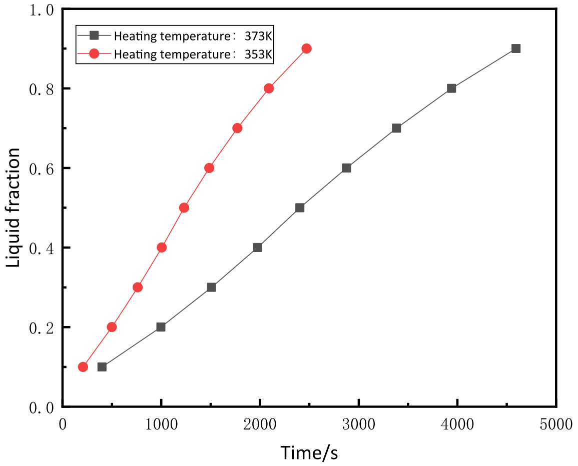

Fig. 4. Liquid fraction for square-enclosure with different heating temperature.

3.3. Model validation

To solve the momentum and energy equations, the power law differencing scheme and the SIMPLE method for pressure–velocity coupling are used. Also, the PRESTO scheme is adopted for the pressure correction equation [30]. The under-relaxation factors for the velocity components, pressure correction, thermal energy, and liquid fraction are 0.7, 0.3, 1, and 0.9, respectively [30,44]. A residual target of 10^{-5} is used for the continuity, momentum and 10^{-6} energy equations.

Different grid sizes and time steps were first tested to ensure independency of the solution by comparing the melting fraction. A grid size about 8000 elements was selected for square unit and 6500 for shell-tube unit also taking the required computer run time into account, the time steps for both are 0.05s. The 300 iterations are sufficient for the convergence requirements.

Because of the complexity of experimental verification and associated uncertainties, we used here comparison to results from the literature. A computational study on the outer surface of a spherical capsule at constant temperature was conducted using the case of Tan et al. [45] to compare with their computational results. The verification run is shown in Fig. 4, which shows good agreement between the two models.

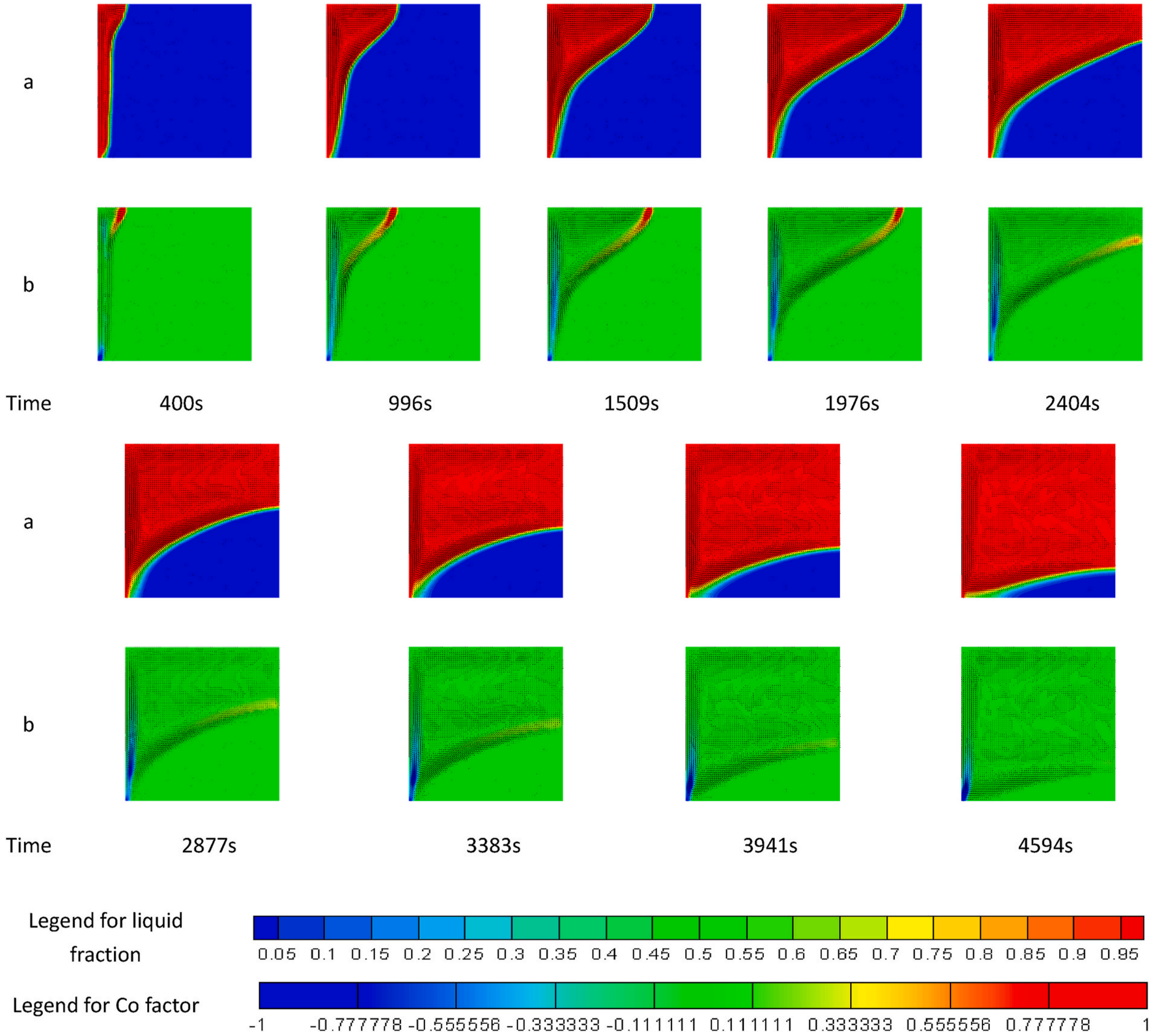

Fig. 5. (a). Liquid fraction (10–90%), Co distribution and corresponding melting times with flow field distributions in the melting process in a square-shaped enclosure (Paraffin) (T_w = 353 K). (b). Liquid fraction (10–90%), Co distribution and corresponding melting times with flow field distributions in the melting process in a square-shaped enclosure (Paraffin) (T_w = 373 K).

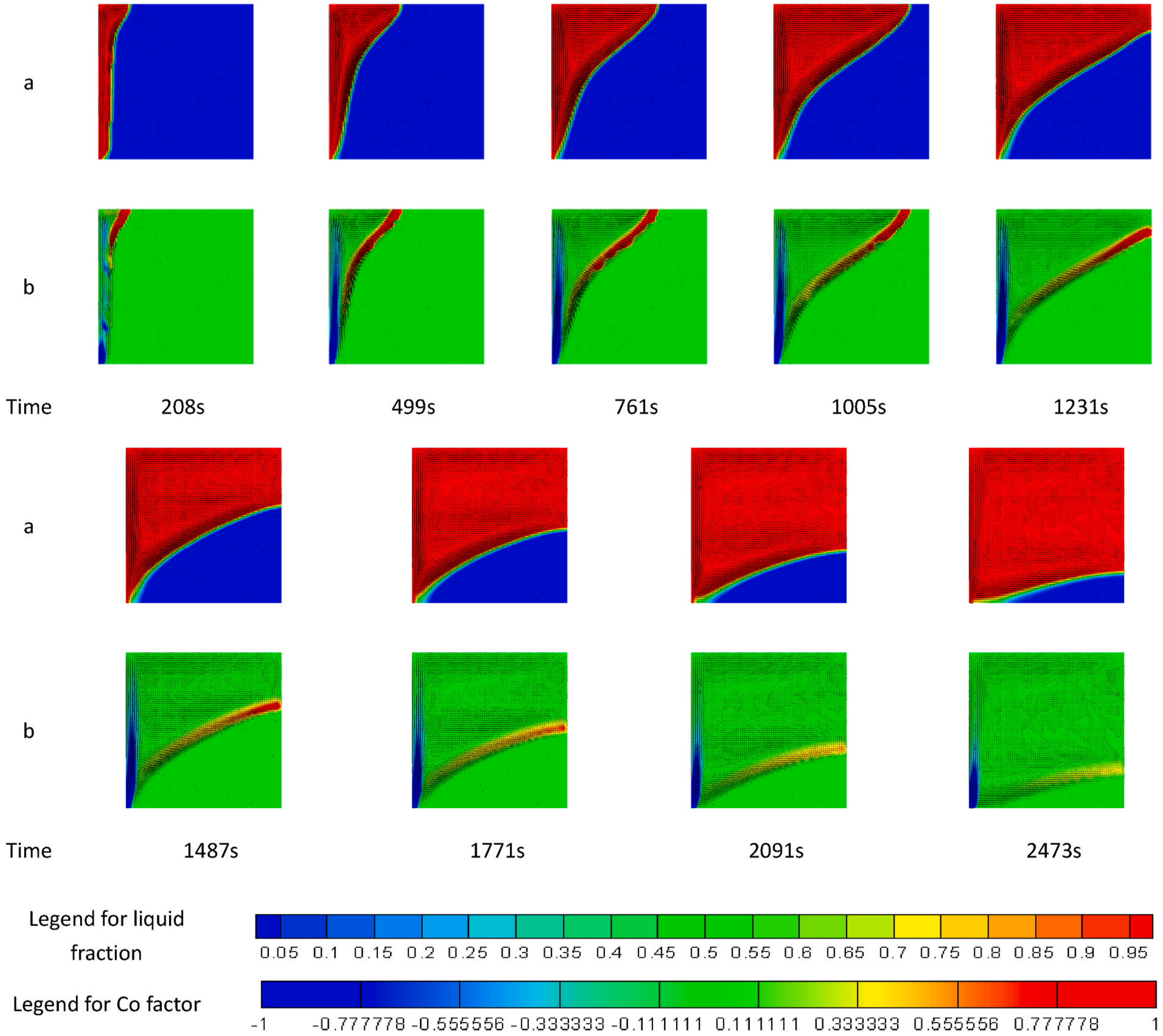

Fig. 5. (*continued*).

4. Results and discussion

4.1. Analysis of melting process in square-shaped enclosure

Fig. 4 show the liquid fraction for square-enclosure with different heating temperature, the melting process time is greatly reduced due to the increase of heating temperature. Fig. 5(a) and (b) show the contour of liquid fraction in line a, Co distribution in line b (from 10% to 90%) and the corresponding heating time in the square enclosure (parameters as in Table 1, geometry defined in Fig. 2(a)). The phase change materials heated at different temperatures have very similar interface profile in the same liquid fraction. However, with lower temperature heating, the mushy zone in lower left corner is thicker than with higher temperature. With a higher heating temperature, it takes less time to reach a certain liquid fraction than with a lower temperature.

As the top of the PCM melts faster than the bottom, it is generally explained that natural convection has a significant effect on the shape of the solid–liquid interface, i.e. the hot liquid flows to the upper part while the cold liquid flows to the lower part [16,41]. However, at the interface this explanation is not fully valid and therefore the Co-factor was introduced to better explain the situation at the interface. To compare the differences for the two heating temperature cases, Co was limited to (−1 K/s, +1 K/s). In the square enclosure, the maximum of Co is on the top and the minimum is in the lower left corner in different heating temperature, that's why the top melts faster while the lower left corner hardly melts. The maximum and the range of maxima first remain almost unchanged and then gradually decrease with increasing of the liquid fraction, and that's why the melting rate decrease with increasing of the liquid fraction. It is worth noting that the minimum of Co always remains in the lower left corner, that's why the lower left corner almost unmelt, even though the heating temperature increases, it should melt as a result of heat conduction. The temperature gradient in the interface and buoyancy will also increase when the heating temperature increases, thus the maximum Co and its distribution range is larger and wider. Interestingly, the Co-factor higher than 0 (in red) has a longer range alongside the solid-liquid interface with higher heating temperature, that's gives the reason why the interface looks more "smooth" while the other have obvious "turning" in the early melting stage. But because the shape of the enclosure is not changing, and thus the interface of the same liquid fraction at different heating temperature is similar. The Co-factor distribution in the liquid zone reflects the intensity of natural convection. In the liquid region near the left wall, Co is lower than 0 parallel to the wall. The minimum value and range decreases with increasing heating temperature, as it improves the natural convection intensity. The non-uniform melting of the upper and lower parts also shows that the main heat source for melting is the temperature boundary layer in the liquid phase region of the interface.

Therefore, the Co-factor gives a well data-based explanation for the PCM melting in square enclosure affected by natural convection. The fundamental reason for the shape of melting front lies in the relationship between the direction of natural convection and temperature gradient in the temperature boundary layer along the solid-liquid interface. The value and distribution of Co-factor also illustrate that not all natural convection promotes melting and the enhancement is also limited.

4.2. Analysis of melting process in shell-tube unit

The other case is the shell-tube heat storage analyzed at the same temperature as the square-shaped case. The case is not simulated according to the symmetric. Fig. 6 show the liquid fraction for shell tube unit with different model, the melting rate almost constant in the eccentric unit while the melting rate is slower and slower in concentric unit. Fig. 7(a) and (b) show the contour of liquid fraction in line a, Co distribution in line b (10%–90%) and the corresponding heating times in the shell-tube unit. Because of the inhomogeneity of the natural convection flow field, the result can not show the symmetrical result, which can be explained in the following Co-factor distribution figure. The eccentric unit melts much faster than the concentric one, and the difference is more pronounced when approaching higher melting fractions. This clearly indicates that the melting rate increases when the inner heating tube moves downwards from the center, which is well in line with previous researches [29–31] providing as explanation natural convection dominated area become larger, but not providing which factor of natural convection plays a crucial role in the melting.

The minimum and the maximum of Co is limited to [−5 K/s, +5 K/s]. Fig. 7(a) shows the range of Co-factor, which first increases, then remains stable, after which it decreases with increasing liquid fraction. This is also demonstrated by the time it takes to melt a 10%-unit of the solid phase PCM. The Co-factor almost 0 when liquid fraction is 70%, this phenomenon shows that natural convection has almost no effect on melting and heat conduction takes dominated in this period. It can be seen that the Co-factor higher than 0 is distributed on both sides and the Co-factor is almost 0 under the heating tube comparing the liquid fraction of 50% and 60%, which is why the melting front changes mainly on both sides when the liquid fraction changes from 50% to 60%. The PCM melts faster when Co factor higher than 0 in the interface while melts slower when Co less than 0, therefore, the melting of PCM is affected by natural convection and accumulated gradually, resulting in asymmetric melting interface.

Fig. 7(b) shows that the Co-factor distribution at the interface demonstrates superiority of the eccentric case over the concentric one during the whole melting time, as the Co-factor higher than 0 appears earlier and lasts a longer time and is more widely distributed in the eccentric case, especially in the later stage of melting. The distribution of Co in the liquid phase also indicates enhancement of natural convection. They have the same heating temperature in concentric and eccentric tubes, but they have very different complete melting times, the value and distribution of Co-factor are the reasons for this phenomenon. Because of the upward movement of the heat flux caused by the buoyancy, the velocity of natural convection is better utilized by moving downwards the inner heating tube, that is, enhancing the cooperation between the direction of natural convection and the temperature gradient. This results are also consistent with that in the square enclosure, the larger the Co-factor value, the faster the PCM melts; the wider the range of Co-factor, the longer the existence time, the faster the melting rate. As for the unsymmetrical interface, this phenomenon is more obvious in

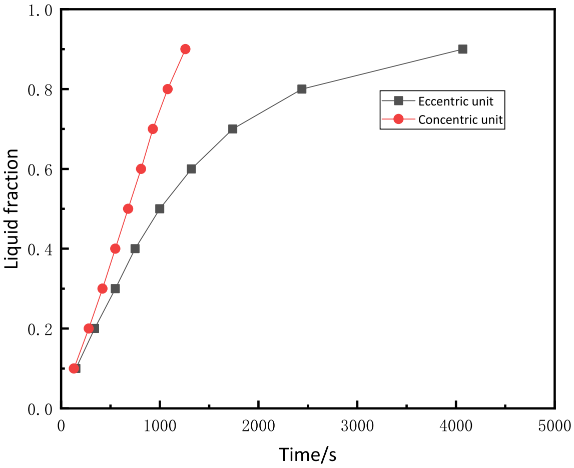

Fig. 6. Liquid fraction for shell-tube unit with different model.

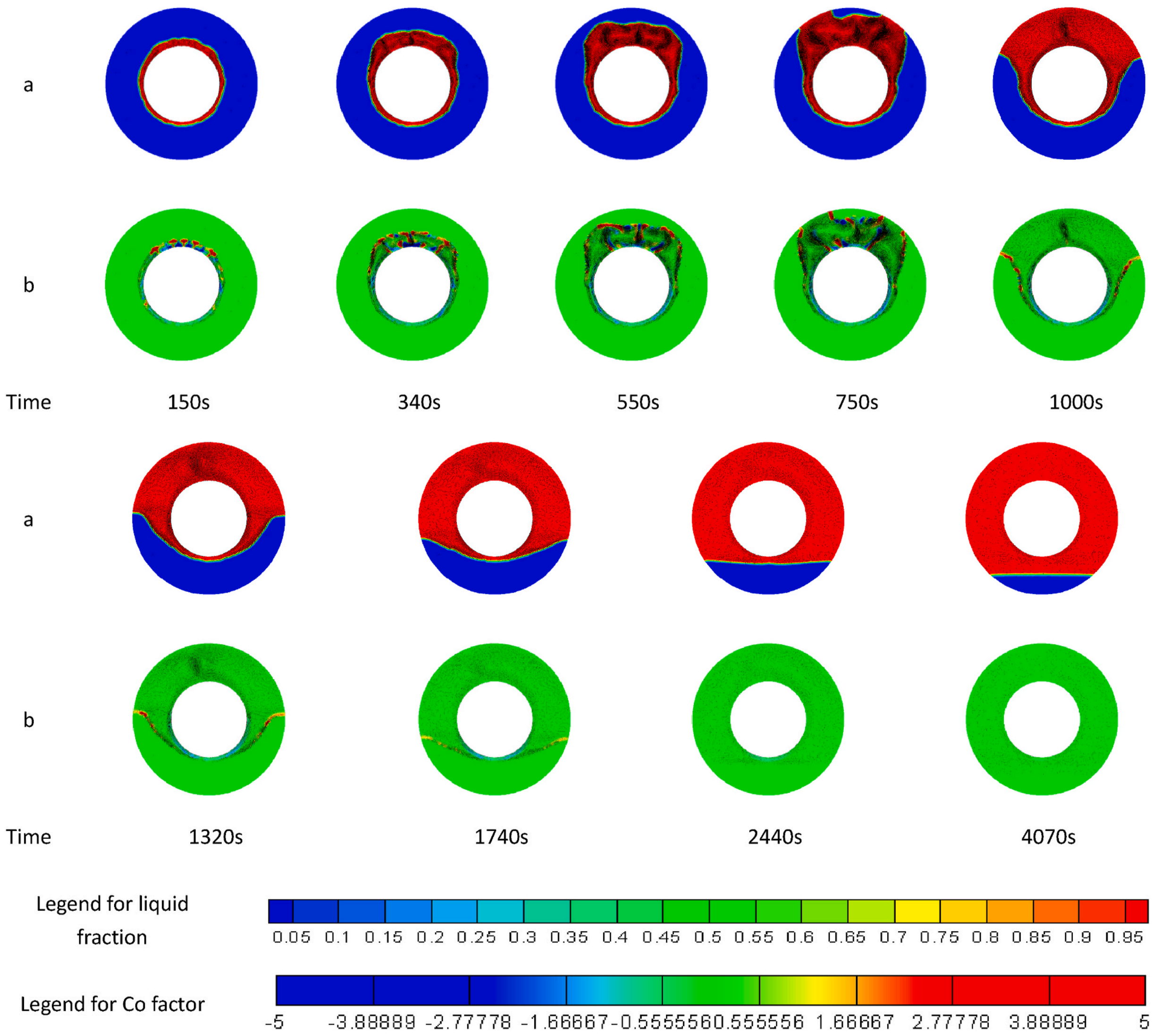

Fig. 7. (a). Liquid fraction (10–90%), Co distribution and corresponding melting times with flow field distributions in the melting process in shell-tube unit (N-eicosane) (concentric, $T_w = 338$ K). (b). Liquid fraction (10–90%), Co distribution and corresponding melting times with flow field distributions in the melting process in shell-tube unit (N-eicosane) (eccentric, $T_w = 338$ K).

eccentric case because the non-uniformity of flow results in the non-uniform distribution of Co and the non-uniformity of Co distribution results in the difference of melting speed of PCM. It can be seen in Fig. 7(b) that PCM where melts faster usually has higher Co while where melts slower has lower Co. Combined with the flow filed, the place near the interface with the velocity toward the interface usually have higher Co while velocity reversal interface have lower Co.

5. Conclusions

In this study, a theoretical framework of the temperature boundary layer and field synergy was developed to explain factors influencing PCM melting affected by natural convection quantitatively analyzing when and how natural convection promotes melting and the effects of natural convection on the melting process are detail distinguished. The results also indicate that the main heat source of solid melting comes from the temperature boundary layer of the solid-liquid interface. Here are main conclusions of this research:

(1) In the direction of natural convection flow, the melting speed of solid phase change materials is faster in different models. This phenomenon is explained by mathematical model in this paper.
(2) The key parameters are extracted from the mathematical model, that is, the magnitude of velocity, velocity direction and temperature gradient.

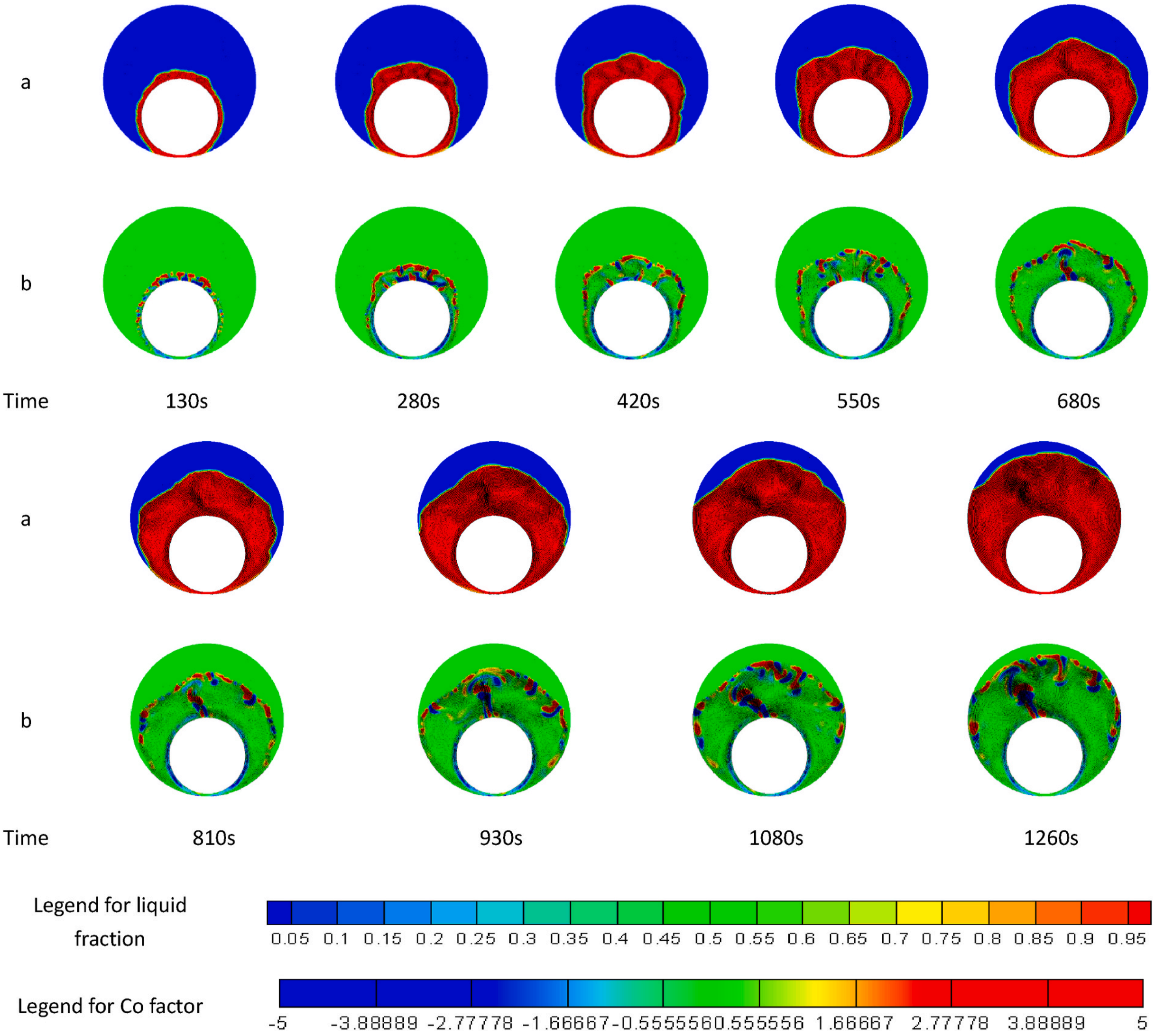

Fig. 7. (*continued*).

(3) The dot product of natural convection velocity and temperature gradient (Co) is the driving force for the melting of solid phase change materials. The Co factor gives well explanation for the non-uniformity of the melting front, increasing the heating temperature or changing the system layout can increase the melting rate of PCM in theory.

The value of Co-factor can clearly show the melting situation and the Co-factor distribution also makes us realize that most of the natural convection does not have a good effect on melting. For further research, it can be pointed out that a new analysis mode can be obtained through the Co-factor, that is, changing the distribution of natural convective flow field can promote the hanging process. Of course, the Co-factor can also make a detailed analysis on the role of fins in the latent heat storage system, because the flow field is changed due to fin. Obviously, Co is an instantaneous quantity, thus, it cannot provide optimize before the melting process is clear.

Authorship contribution statement

Bingkun Huang: Methodology, Conceptualization, Validation, Writing – original draft. Shimi Yang: Methodology, Formal analysis, Writing – review & editing. Enyi Hu: Formal analysis, Methodology, Conceptualization. Xiuxiu Li: Formal analysis, Methodology, Conceptualization. Jun Wang: Resources, and, Project administration. Peter D. Lund: Original Editing.

Declaration of competing interest

The authors declare that they have no known competing financial interests or personal relationships that could have appeared to influence the work reported in this paper.

Acknowledgement

This study was supported by "the Fundamental Research Funds for the Central Universities"(Grand No. 2242021k30028). This work was partially supported by Aalto University.

References

[1] A. Sharma, V.V. Tyagi, C.R. Chen, D. Buddhi, Review on thermal energy storage with phase change materials and applications, Renew. Sustain. Energy Rev. 13 (2009) 318–345.
[2] H. Ibrahim, A. Ilinca, J. Perron, Energy storage systems - characteristics and comparisons, Renew. Sustain. Energy Rev. 12 (2008) 1221–1250.
[3] S. Chavan, V. Gumtapure, D. Ap, Numerical and experimental analysis on thermal energy storage of polyethylene/functionalized graphene composite phase change materials, J. Energy Storage 27 (2020) 101045.
[4] S. Chavan, V. Gumtapure, D. Arumuga Perumal, Characterization of linear low-density polyethylene with graphene as thermal energy storage material, Mater. Res. Express 6 (2019), 065511.
[5] C. Santosh, G. Veershetty, A.P. Dharmaraj, A review on thermal energy storage using composite phase change materials, Recent Pat. Mech. Eng. 11 (2018) 298–310.
[6] S. Chavan, V. Gumtapure, D.A. Perumal, Preparation and characterization of nanoparticle blended polymers for thermal energy storage applications, in: 2nd International Conference on Polymer Composites (ICPC). Natl Inst Technol Karnataka, Dept Mech Engn, Surathkal, INDIA, 2018.
[7] S. Chavan, V. Gumtapure, D.A. Perumal, Preparation of functionalized graphene-linear low-density polyethylene composites by melt mixing method 2247 (2020), 040010.
[8] C. Santosh, G. Veershetty, D.A. Perumal*, Performance assessment of composite phase change materials for thermal energy storage-characterization and simulation studies, Recent Pat. Mech. Eng. 14 (2021) 75–85.
[9] N.S. Dhaidan, J.M. Khodadadi, Melting and convection of phase change materials in different shape containers: a review, Renew. Sustain. Energy Rev. 43 (2015) 449–477.
[10] A. El-Sawi, F. Haghighat, H. Akbari, Assessing long-term performance of centralized thermal energy storage system, Appl. Therm. Eng. 62 (2014) 313–321.
[11] M.M. Joybari, F. Haghighat, J. Moffat, P. Sra, Heat and cold storage using phase change materials in domestic refrigeration systems: the state-of-the-art review, Energy Build. 106 (2015) 111–124.
[12] R. Baetens, B.P. Jelle, A. Gustavsen, Phase change materials for building applications: a state-of-the-art review, Energy Build. 42 (2010) 1361–1368.
[13] A. Najafian, F. Haghighat, A. Moreau, Integration of PCM in domestic hot water tanks: Optimization for shifting peak demand, Energy Build. 106 (2015) 59–64.
[14] P. Lamberg, Approximate analytical model for two-phase solidification problem in a finned phase-change material storage, Appl. Energy 77 (2004) 131–152.
[15] J.M. Mahdi, S. Lohrasbi, E.C. Nsofor, Hybrid heat transfer enhancement for latent-heat thermal energy storage systems: a review, Int. J. Heat Mass Tran. 137 (2019) 630–649.
[16] H. Shokouhmand, B. Kamkari, Experimental investigation on melting heat transfer characteristics of lauric acid in a rectangular thermal storage unit, Exp. Therm. Fluid Sci. 50 (2013) 201–212.
[17] N.H.S. Tay, F. Bruno, M. Belusko, Comparison of pinned and finned tubes in a phase change thermal energy storage system using CFD, Appl. Energy 104 (2013) 79–86.
[18] K. Lafdi, O. Mesalhy, S. Shaikh, Experimental study on the influence of foam porosity and pore size on the melting of phase change materials, J. Appl. Phys. 102 (2007) 6.
[19] C.J. Ho, J.Y. Gao, An experimental study on melting heat transfer of paraffin dispersed with Al2O3 nanoparticles in a vertical enclosure, Int. J. Heat Mass Tran. 62 (2013) 2–8.
[20] S. Chavan, V. Gumtapure, D. Arumuga Perumal, Computational investigation of bounded domain with different orientations using CPCM, J. Energy Storage 22 (2019) 355–372.
[21] Y.B. Tao, Y.K. Liu, Y.L. He, Effects of PCM arrangement and natural convection on charging and discharging performance of shell-and-tube LHS unit, Int. J. Heat Mass Tran. 115 (2017) 99–107.
[22] J.L. Xie, K.F. Choo, J.H. Xiang, H.M. Lee, Characterization of natural convection in a PCM-based heat sink with novel conductive structures, Int. Commun. Heat Mass Tran. 108 (2019) 13.
[23] M. Sheikholeslami, S. Lohrasbi, D.D. Ganji, Numerical analysis of discharging process acceleration in LHTESS by immersing innovative fin configuration using finite element method, Appl. Therm. Eng. 107 (2016) 154–166.
[24] M.J. Hosseini, A.A. Ranjbar, K. Sedighi, M. Rahimi, A combined experimental and computational study on the melting behavior of a medium temperature phase change storage material inside shell and tube heat exchanger, Int. Commun. Heat Mass Tran. 39 (2012) 1416–1424.
[25] K.W. Ng, Z.X. Gong, A.S. Mujumdar, Heat transfer in free convection-dominated melting of a phase change material in a horizontal annulus, Int. Commun. Heat Mass Tran. 25 (1998) 631–640.
[26] M.M. Farid, A.K. Mohamed, Effect of natural-convection on the process of melting and solidification of paraffin wax, Chem. Eng. Commun. 57 (1987) 297–316.
[27] M. Farid, Y. Kim, T. Honda, A. Kanzawa, The role of natural-convection during melting and solidification of PCM in a vertical cylinder, Chem. Eng. Commun. 84 (1989) 43–60.
[28] M.M. Joybari, F. Haghighat, S. Seddegh, Natural convection characterization during melting of phase change materials: development of a simplified front tracking method, Sol. Energy 158 (2017) 711–720.
[29] X.L. Cao, Y.P. Yuan, B. Xiang, F. Haghighat, Effect of natural convection on melting performance of eccentric horizontal shell and tube latent heat storage unit, Sust Cities Soc 38 (2018) 571–581.
[30] A.R. Darzi, M. Farhadi, K. Sedighi, Numerical study of melting inside concentric and eccentric horizontal annulus, Appl. Math. Model. 36 (2012) 4080–4086.
[31] M.Y. Yazici, M. Avci, O. Aydin, M. Akgun, Effect of eccentricity on melting behavior of paraffin in a horizontal tube-in-shell storage unit: an experimental study, Sol. Energy 101 (2014) 291–298.
[32] Z. Rui, J. Li, J. Ma, H. Cai, B. Nie, H. Peng, Comparative study on natural convection melting in square cavity using lattice Boltzmann method, Result. Phys. 18 (2020) 103274.
[33] S. Yang, B. Huang, J. Wang, P.D. Lund, Characteristics of natural convection in n-eicosane in a square cavity with discrete heat source, Case Stud. Therm. Eng. 27 (2021) 101245.
[34] W. Li, H. Wan, P. Zhang, P. Liu, G. He, F. Qin, A method to evaluate natural convection heat transfer in microencapsulated phase change material (MPCM) slurry: an experimental study, Int. Commun. Heat Mass Tran. 96 (2018) 1–6.
[35] A. Parida, A. Bhattacharya, P. Rath, Effect of convection on melting characteristics of phase change material-metal foam composite thermal energy storage system, J. Energy Storage 32 (2020) 101804.
[36] Z.Y. Guo, D.Y. Li, B.X. Wang, A novel concept for convective heat transfer enhancement, Int. J. Heat Mass Tran. 41 (1998) 2221–2225.
[37] W.Q. Tao, Z.Y. Guo, B.X. Wang, Field synergy principle for enhancing convective heat transfer-its extension and numerical verifications, Int. J. Heat Mass Tran. 45 (2002) 3849–3856.
[38] W.Q. Tao, Y.L. He, Q.W. Wang, Z.G. Qu, F.Q. Song, A unified analysis on enhancing single phase convective heat transfer with field synergy principle, Int. J. Heat Mass Tran. 45 (2002) 4871–4879.

[39] A.S. Bejan, F. Bode, T. Catalina, C. Teodosiu, Mesh independency study for an elementary perforated panel part of an air solar collector, in: M.C. Balan, F. Bode, C. Croitoru, A. Dogeanu, A. Georgescu, C. Georgescu, et al. (Eds.), Sustainable Solutions for Energy and Environment, Cedex A: E D P Sciences, 2019.

[40] M. Jourabian, M. Farhadi, A.A.R. Darzi, Outward melting of ice enhanced by Cu nanoparticles inside cylindrical horizontal annulus: lattice Boltzmann approach, Appl. Math. Model. 37 (2013) 8813–8825.

[41] A.V. Arasu, A.S. Mujumdar, Numerical study on melting of paraffin wax with Al2O3 in a square enclosure, Int. Commun. Heat Mass Tran. 39 (2012) 8–16.

[42] M. Kumar, D.J. Krishna, Influence of mushy zone constant on thermohydraulics of a PCM, in: B.K. Choudhury, S.K. Rout, P. Muthukumar, R.K. Sahoo, S.S. Sahoo (Eds.), International Conference on Recent Advancement in Air Conditioning and Refrigeration, Raar 2016, Elsevier Science Bv, Amsterdam, 2017, pp. 314–321.

[43] S. Wu, Experimental and Numerical Simulation Study on Phase Change Heat Transfer Enhancement of Nanocomposite Heat Storage Materials [D], South China University of Technology, 2010.

[44] Y.P. Yuan, X.L. Cao, B. Xiang, Y.X. Du, Effect of installation angle of fins on melting characteristics of annular unit for latent heat thermal energy storage, Sol. Energy 136 (2016) 365–378.

[45] F.L. Tan, S.F. Hosseinizadeh, J.M. Khodadadi, L.W. Fan, Experimental and computational study of constrained melting of phase change materials (PCM) inside a spherical capsule, Int. J. Heat Mass Tran. 52 (2009) 3464–3472.